RF COUPLING CHOICES, POWER REQUIREMENTS, AND IMPACT ON TRANSIENTS IN THE PERLE ENERGY RECOVERY LINAC*

F. Bouly†, Université Grenoble Alpes, CNRS/IN2P3, Grenoble INP, LPSC, Grenoble, France
N. Belouchrani, C. Joly, R. Roux, Université Paris-Saclay, CNRS/IN2P3, IJCLab, Orsay, France
On behalf of the PERLE collaboration

Abstract

The PERLE project aims to construct a novel high power Energy Recovery Linac (ERL) demonstrator (5 MW) for developing and applying the energy recovery technique in a multi-turn configuration. In its final layout the machine will operate in a three turn mode, delivering a 20 mA electron beam at 250 MeV. These challenging parameters make PERLE a unique multi-turn ERL facility in an unexplored power regime, enabling the study of accelerator phenomena and paving the way for future large-scale ERLs. To achieve maximum efficiency, dedicated RF studies have been carried out to dimension the RF system, with particular focus on the external coupling of the superconducting cavities in both the injector and the ERL sections. These studies enable the determination of the required RF power and provide a first evaluation of transient effects on the RF system.

RF REQUIREMENTS

PERLE Cryomodules

The PERLE project aims to construct a novel high-power Energy Recovery Linac (ERL) demonstrator (5 MW) for developing and applying the energy recovery technique in a multi-turn configuration. In its final layout, the machine will operate in a three-turn mode, delivering a 20 mA electron beam at 250 MeV (cf. Fig. 1) [1, 2].

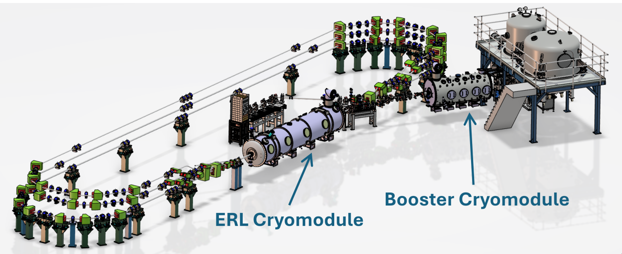

Figure 1: PERLE accelerator & cryomodules layout [3].

The Booster cryomodule, located in the injector [4] part, enables acceleration of the beam from the Electron DC Gun (kinetic energy of 350 keV) [5, 6] up to 7 MeV (total energy) with four single-cell cavities. The ERL cryomodule, composed of four 5-cell cavities, which enables both the acceleration (up to 250 MeV after 3 passes) and deceleration process (down back to 7 MeV after 6 passes) for power recovery. The main characteristics of the cavities that compose these modules are summarised in Table 1.

Table 1: Main RF parameters of the PERLE cryomodules

	Cryomodule	
Parameter	**Booster**	**ERL**
No. of cavities / cryomodule	4	
Frequency [MHz]	801.58	
β_{opt}	1	
r/Q [Ω]	109	523
L_{acc} [m]*	0.187	0.935
V_c [MV]	1.4–1.8	20.5
Synchronous phase [°]	−25–25	0
Q_0	1.0×10^{10}	3.0×10^{10}
P_{cav} [W]	3 (max.)	26.7
Q_t	4.0×10^{11}	8.0×10^{12}

*With $L_{acc} = N_{gap}\beta_{opt}\lambda/2$.

Beam dynamics requirements directly impact RF system specifications, in particular stability criteria for frequency, accelerating field amplitude, and phase. Sustainability considerations further require minimising energy consumption and RF power, leading to a trade-off between cavity bandwidth, sensitivity to perturbations, reliability, and maintainability. In addition, specific operating modes (e.g. commissioning) may require pulsed operation or a wider dynamic range than nominal conditions. These constraints have been taken into account to define the coupling of the Fundamental Power Coupler (FPC) for both cryomodules and to optimise the overall power balance.

RF Power and Definitions Reminder

In steady-state operation, the RF forward power (P_{fwd}) required from the amplifier to drive a superconducting cavity can be expressed as:

$$P_{fwd} = \frac{V_c^2 Q_{ext}}{4(r/Q)Q_L^2}\left[\left(1 + \frac{I_{b0}(r/Q)Q_L\cos(\phi_s)}{V_c}\right)^2 + \left(2Q_L\frac{\Delta f}{f} + \frac{I_{b0}(r/Q)Q_L\sin(\phi_s)}{V_c}\right)^2\right]. \quad (1)$$

It depends on the cavity set points (accelerating voltage V_c and synchronous phase ϕ_s), the beam current I_{b0}, the cavity shunt impedance (r/Q), the frequency detuning Δf, the FPC coupling Q_{ext}, and the loaded quality factor Q_L, defined as:

$$\frac{1}{Q_L} = \frac{1}{Q_0} + \frac{1}{Q_{ext}} + \frac{1}{Q_t}, \quad (2)$$

* Part of this work is supported by the ANR under the France 2030 framework, ref. ANR-24-RRII-0001, and by the European Union's HORIZON-INFRA-2023-TECH-01-01 programme under GA No. 101131435.
† frederic.bouly@lpsc.in2p3.fr

where Q_t is the coupling of the pick-up antenna and Q_0 the cavity quality factor. Minimising P_{fwd} requires adjusting the cavity detuning to its optimal value (Eq. (3)):

$$\Delta f_{opt} = -\frac{I_{b0}(r/Q)\sin(\phi_s)}{2V_c} f. \quad (3)$$

In this optimal condition, Eq. (1) becomes:

$$P_{fwd}(\Delta f_{opt}) = \frac{V_c^2 Q_{ext}}{4(r/Q)Q_L^2}\left(1 + \frac{I_{b0}(r/Q)Q_L\cos(\phi_s)}{V_c}\right)^2. \quad (4)$$

BOOSTER CAVITIES

Based on Eq. (4) one can evaluate the variation of the minimum required amplifier power as a function of the coupling. This is given for each cavity of the Booster, which will not operate at the same accelerating voltage and synchronous phase, as this is determined according to beam dynamics optimisation [7]. For instance, acceleration in cavity #1 is much smoother than in cavity #4 (which may require more RF power). To provide an order of magnitude, the case where each cavity provides the same energy gain with on-crest acceleration (i.e. $V_c = 1.5\,MV$ and $\phi_s = 0°$) is also plotted.

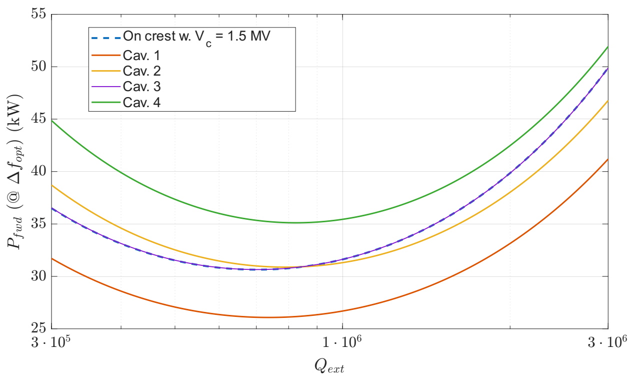

Figure 2: P_{fwd} as function of Q_{ext} for different cavity tuning.

To determine the optimal coupling, the evolution of the RF power as a function of beam current was also considered. Indeed, Phase 1 of the PERLE project aims to operate with a 5 mA beam, with a subsequent increase in beam current during the second commissioning phase. Fig. 3 shows the evolution of the minimum required RF power for cavity #4 -the most demanding case - as a function of beam current.

According to the project staging strategy, it was then chosen to operate with $Q_{\mathrm{ext,\,Booster}} = 1.7\ 10^6$. The cavity bandwidth would then be 471 Hz, which makes the system quite safe with regard to microphonic perturbations. This coupling value would thus allow the Booster to operate during Phase 1 ($I_{b0} = 5$ mA), using amplifiers with a power of ~10 kW (depending on the cavity position and including margins for errors, attenuation, etc.) [8]. However, to accommodate higher beam currents, modular amplifiers are required, enabling future power upgrades. At 20 mA, excess power consumption is expected (more than 5 kW for the most demanding cavity), but mitigation strategies are considered:

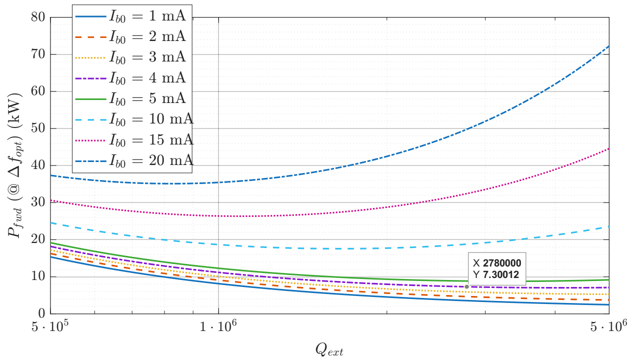

Figure 3: P_{fwd} as function of Q_{ext} and beam current for the tuning of cavity #4 (cf. Fig. 2).

adjusting the FPC antenna or impedance matching in the upstream RF transmission line [8].

ERL CAVITIES

For the ERL cavities, the situation can be described as follows. They will "see" a bunch passing through them 6 times, but at different energies or RF phases: 3 times on-crest acceleration ($\phi_s = 0°$) and 3 times off-crest deceleration ($\phi_s = 180°$). Following the PERLE beam-filling pattern in steady state [1], accelerated and decelerated bunches are distributed alternately. One can therefore consider that a cavity sees 6 different 20 mA beams. Thus, in steady-state conditions, assuming perfect synchronism and beam trajectories, the cavity experiences an overall zero current beam loading (cf. Fig. 6).

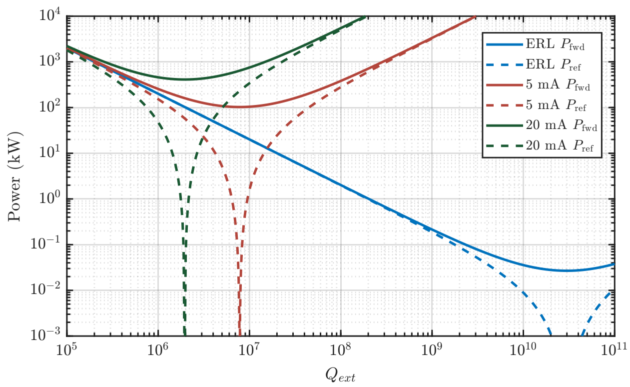

Figure 4: P_{fwd} and P_{ref} as a function of Q_{ext} for ERL operation compared with conventional acceleration at beam currents of 5 mA and 20 mA.

Consequently, using Eq. 4 and Table 1 parameters, Fig. 4 presents the minimum required power to operate in 'ERL mode' as a function of Q_{ext}. The expected reflected power (P_{ref}) is also plotted. To quantify the power gain compared with standard acceleration, two additional cases are presented: 20 mA and 5 mA beam acceleration. It is found that the optimal coupling for ERL mode operation corresponds to critical coupling ($Q_{\mathrm{ext}} = Q_0$). In principle, this would reduce RF power consumption to only a few tens of watts. However, such coupling results in an extremely narrow system bandwidth, below 1 Hz, making LLRF control impractical. External coupling is therefore set by the minimum acceptable bandwidth required for stable RF control. Frequency perturbations (e.g. microphonics) also affect RF power consumption, as illustrated in Fig. 5. A bandwidth of ~100 Hz represents a reasonable compromise, although challenging. Still, the detuning error must remain below ~20 Hz to ensure RF power stays under 40 kW (maximum planned power available per cavity) [8].

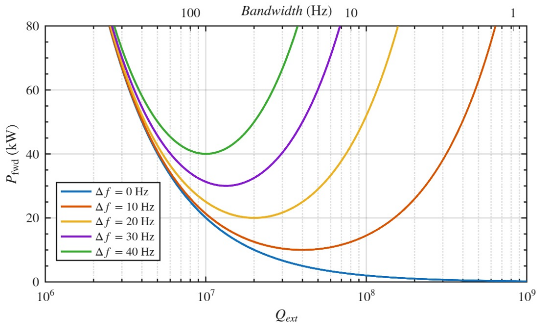

Figure 5: Effect of frequency detuning (e.g. microphonics) on RF power consumption as a function of coupling, for ERL operation mode.

For the PERLE ERL cryomodule, cavity frequency tuning is achieved using a cold tuning system based on a motor drive and piezoelectric actuators. The external quality factor chosen to obtain is then : $Q_{ext,\mathrm{ERL}} = 8\ 10^6$. At optimal detuning ($\Delta f = 0$ Hz), the minimum RF power would therefore be 25.1 kW.

TRANSIENTS EFFECT

The coupling choice and maximum RF drive power for the ERL cryomodule have been established mainly under steady-state conditions, assuming ideal beam recirculation synchronicity. However, dynamic loading due to incomplete energy recovery must be considered for operation and RF power margins [9]. In some machines, this arises from unintentional errors on the energy-recovered beam, such as path-length errors in large-scale systems; therefore, correction systems are required, as foreseen for PERLE [10]. RF drive requirements in ERLs are, however, not only governed by steady-state conditions but also by beam transients, including the filling pattern [11], as well as environmental and design effects such as microphonics. For this purpose, FE-FRT systems represent a promising technology [12] to improve performance, reduce RF power consumption, and mitigate instability risks during transients. The impact of transients on RF systems must therefore be evaluated, particularly during beam-on and beam-off operation. When the beam is injected into the ERL, strong beam-loading transients occur, as illustrated in Fig. 6, for a 2 µs macropulse at 20 mA (80 bunches).

Due to strong beam loading during these transients, the capabilities of the PERLE RF system must be evaluated in order to maintain field stability in the cavities according to the available power margins. For this purpose, a superconducting cavity model, including its associated control loops

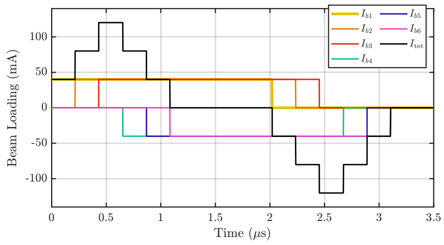

Figure 6: Beam loading experienced by an ERL cavity during the injection of a 2 µs macropulse at 20 mA (80 bunches at 40 MHz).

(LLRF and tuning system), is being developed. This model is based on previous developments [13] and was benchmarked on other superconducting linac operation [14].

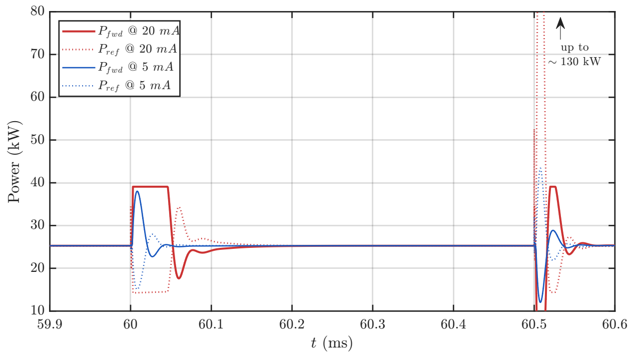

Figure 7: Cavity power transients during the injection of a 500 µs pulse (20 mA or 5 mA) in the PERLE ERL.

The Fig. 7 shows the transient evolution of P_{fwd} and P_{ref} when a macropulse of 0.5 ms is injected, comparing both cases of beam current at 20 mA and 5 mA. It is assumed that the cavity is at optimal detuning for steady-state operation, and the maximum available RF power is 40 kW [8]. These preliminary results indicate that injecting higher beam current may induce amplifier saturation, with a risk of losing LLRF control. Another transient issue occurs during "unloading" of the machine, when only the decelerated beams remain, leading to a strong peak power that may need to be evacuated through the FPC port and an RF circulator. Such events may also occur when the beam has to be stopped by the machine protection system. While loading transients may be mitigated — for instance, by ramping up the beam current from injection and implementing LLRF feedforward — unloading transients require properly designed RF protection systems.

CONCLUSION

The coupling values for the cavities of both cryomodules have been established ($Q_{\mathrm{ext,\ Booster}} = 1.7\ 10^6$ & $Q_{\mathrm{ext,\ ERL}} = 8.0\ 10^6$). A model (cavity and feedback control loops) has been developed to assess the impact of transients. Further studies will be carried out to identify potential limitations and to properly design the RF system, as well as to define operational procedures to mitigate these effects.

REFERENCES

[1] A. Fomin *et al.*, “Beam dynamics challenges and optics development for the PERLE multi-turn ERL”, presented at IPAC’26, Deauville, France, May 2026, paper WEO5M01, this conference.

[2] J. Michaud *et al.*, “Status of the beam dynamics studies for the PERLE Energy Recovery Linac”, in *Proc. IPAC’25*, Taipei, Taiwan, Jun. 2025, pp. 702–705. doi:10.18429/JACoW-IPAC2025-MOPS041

[3] S. Marchal and S. Brault, IJCLab, CNRS, France, private communication, 2025.

[4] R. Roux *et al.*, “Status of the PERLE injector”, presented at IPAC’26, Deauville, France, May 2026, paper WEP5090, this conference.

[5] M. Baylac *et al.*, “High current photogun for the Energy Recovery Linac PERLE”, presented at IPAC’26, Deauville, France, May 2026, paper THP2104, this conference.

[6] M. De Vos *et al.*, “High quantum efficiency alkali-antimonide photocathodes for PERLE high current DC gun”, presented at IPAC’26, Deauville, France, May 2026, paper THP2102, this conference.

[7] C. I. D. Monaghan *et al.*, “Experimental investigation of injector halo for PERLE using scaled measurements at cERL”, presented at IPAC’26, Deauville, France, May 2026, paper THP2108, this conference.

[8] C. Joly *et al.*, “RF system status for PERLE”, presented at IPAC’26, Deauville, France, May 2026, paper WEP6146, this conference.

[9] T. Powers and C. Tennant, “Implications of incomplete energy recovery in SRF-based energy recovery linacs”, in *Proc. ERL’07*, Daresbury, UK, May 2007, pp. 75–79.

[10] J. Issa *et al.*, “Ongoing studies of longitudinal matching for the PERLE accelerator”, presented at IPAC’26, Deauville, France, May 2026, paper SUP5001, this conference.

[11] S. Setiniyaz, R. Apsimon, and P. H. Williams, “Implications of beam filling patterns on the design of recirculating energy recovery linacs”, *Phys. Rev. Accel. Beams*, vol. 23, no. 7, p. 072002, 2020. doi:10.1103/PhysRevAccelBeams.23.072002

[12] I. Ben-Zvi, G. Burt, A. Castilla, A. Macpherson, and N. Shipman, “Conceptual design of a high reactive-power ferroelectric fast reactive tuner”, *Phys. Rev. Accel. Beams*, vol. 27, no. 5, p. 052001, 2024. doi:10.1103/PhysRevAccelBeams.27.052001

[13] I. Martin-Hoyo, F. Bouly *et al.*, “Optimized adaptive control for the MYRRHA linear accelerator: Control system design for a superconducting cavity in a particle accelerator”, *IEEE Control Syst. Mag.*, vol. 38, no. 2, pp. 44–79, 2018. doi:10.1109/MCS.2017.2786420

[14] F. Bouly *et al.*, “Superconducting cavity and RF control loop model for the SPIRAL2 Linac”, in *Proc. LINAC’22*, Liverpool, UK, Aug.–Sep. 2022, pp. 767–770. doi:10.18429/JACoW-LINAC2022-THPOPA13